

A simplified and robust proxy-based approach for overcoming unmeasured confounding in EHR studies

Haley Colgate Kottler haley.kottler@wisc.edu

Department of Mathematics, University of Wisconsin - Madison, Madison, WI, USA

and

Amy Cochran cochran4@wisc.edu

Department of Mathematics and Department of Population Health Sciences,
University of Wisconsin - Madison, Madison, WI, USA

June 17, 2025

Abstract

Electronic health records (EHR) are used to study treatment effects in clinical settings, yet unmeasured confounding remains a persistent challenge. Indirect measurements of the unmeasured confounder (proxies) offer a potential solution, but existing approaches—such as proximal inference or full joint modeling—can be difficult to implement. We propose a two-stage, proxy-based method that is practical, broadly applicable, and robust. In the first stage, we apply factor analysis to proxy and treatment variables, extracting information on latent factors that serve as a surrogate for the unmeasured confounder. In the second stage, we use this model to build covariates that improve causal effect estimation in a standard outcome regression model. Through simulations, we test the method’s performance under assumption violations, including non-normal errors, model misspecification, and scenarios where instruments or confounders are incorrectly treated as proxies. We also apply the method to estimate the effect of hospital admission for older adults presenting to the emergency department with chest pain, a setting where standard analyses may fail to recover plausible effects. Our results show that this simplified strategy recovers more reliable estimates than conventional adjustment methods, offering applied researchers a practical tool for addressing unmeasured confounding with proxy variables.

1 Introduction

Electronic health records (EHR) offer a useful resource for improving clinical decision-making, especially in situations where the best course of action is unclear. However, accurately identifying effective practices requires careful handling of confounding. Traditional guidance recommends adjusting for all variables available prior to treatment. This approach often works well, especially with modern tools, but it can still lead to biased results when important confounders are missing. Even in detailed datasets like EHR, relevant information is often incomplete, making unmeasured confounding fairly common in practice.

Typically, handling unmeasured confounding relies on special situations, such as natural experiments or instrumental variables (IV). When these situations are unavailable, alternative methods become essential. A promising but underutilized strategy leverages indirect measurements (proxies) of the unmeasured confounder. In EHR, such proxies are often available; for example, vital signs may reflect latent traits not directly recorded. Moreover, recent proximal causal inference methods introduced by Tchetgen Tchetgen [2013], Miao et al. [2018], Kuroki and Pearl [2014] provide a compelling theoretical foundation, demonstrating when such proxies can be used to identify causal effects despite unmeasured confounding.

Together, the availability of proxy variables and the existence of supporting theory make this strategy particularly appealing. However, adoption has been limited. This may be due to the technical demands these methods place on the practitioner, such as solving integral equations, modeling via integral operators,

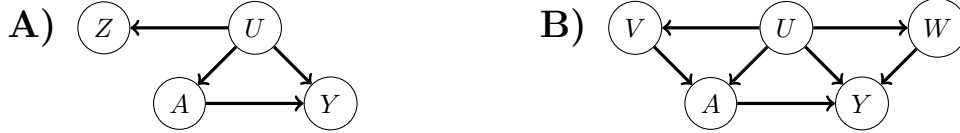


Figure 1: DAGs describing unmeasured confounding: A) with a general proxy variable, B) with a negative control outcome (NCO) and a negative control exposure (NCE).

and categorizing proxies into distinct types. As a result, practitioners may find proximal causal inference difficult to implement.

Another option is to fully model the proxy variables along with the treatment, outcome, and unmeasured confounder. We previously applied this strategy in a series of studies examining hospital admission decisions, and were able to adjust for confounding more thoroughly than standard approaches [Cochran et al., 2019, Alvarez Avendaño et al., 2020, 2022, 2025]. In several cases, this more thorough adjustment reversed conclusions drawn from analyses that relied solely on measured confounders—suggesting that admission was beneficial rather than harmful, results that aligned more closely with clinical expectations. Even so, it was built for a narrow use case (admissions), which made it hard to apply elsewhere and raised reasonable doubts about what would happen if the modeling assumptions were not valid.

Therefore, to support broader adoption of proxy-based adjustment, this paper introduces a simplified proxy-based approach. The method uses a factor analysis model to capture the shared influence of unmeasured confounders on both treatment and proxies. This factor analysis model then helps recover information about the confounding process, which we use to build covariates that improve causal effect estimation in the outcome model. The result is a two-stage procedure that is easy to implement, uses familiar statistical tools (factor analysis and regression), can be broadly applied, and remains robust under common violations.

We illustrate our approach with a real-world problem: hospital admission decisions for older adults with chest pain. Chest pain can reflect something as mild as heartburn, or as severe as a heart attack. Clinicians must decide whether to admit the patient or send them home, a decision that is subtle and difficult because older adults face competing risks. While older patients may benefit from the increased monitoring and quick access to care available in the hospital, they are more likely to experience deconditioning or acquire infections as a result of hospitalization. We can use data from EHR to guide this decision, but unmeasured confounding remains a concern. Fortunately, this may be helped by use of proxy variables.

Our goal is to make proxy-based methods more accessible and practical for EHR-based research, where unmeasured confounding is common and often unavoidable. Specifically, we aim to: (i) propose and analyze a proxy-based procedure for adjusting for unmeasured confounding; (ii) evaluate its robustness under a range of violations using simulated data; and (iii) demonstrate its utility through a case study using EHR data. Section 2 discusses previous innovations using proxy variables. Section 3 introduces a causal framework. In Section 4, we identify the estimand using observed variables. In Section 5, we demonstrate an estimation method. Sections 6 and 7 contain robustness analysis and a case study. Section 8 discusses the results and concludes our analysis.

2 Literature Review

It is common practice to include and adjust for as many pre-treatment covariates as practically possible, since this usually improves models for prediction. However, improper adjustments can actually increase bias in estimates of causal effects. A proxy variable is a type of pre-treatment variable that can be seen as a noisy measurement of the underlying confounding. For example, blood pressure could be a proxy for cardiac health. We denote the treatment by A , the outcome of interest by Y , unmeasured confounders by U , and proxies by V , W or Z depending on their relationship to the other variables, as shown in Figure 1.

Greenland [1980] argued that adjusting by a binary proxy leads to an estimate between the crude estimate and the true value, reducing bias. Ogburn and VanderWeele [2012] later proved that contrary to Greenland’s argument, adjusting for a proxy can lead to estimates that are worse than the unadjusted estimate. They went on to show that if the exposure, confounder, and proxy are all binary, a monotonicity assumption

on $\mathbb{E}[Y|U]$ is enough to guarantee that direct adjustment for a proxy produces better estimates. More recent work has loosened this condition, in contexts where the proxy is conditionally independent of both the exposure and the outcome, given the confounder. This corresponds to Z in Figure 1A. For example, Peña et al. [2021] shows that for discrete or continuous outcome, and categorical proxy and confounder, then under assumptions on the conditional distributions of the treatment and proxy on the confounder, direct adjustment for a proxy decreases error. However, because the conditions under which direct proxy adjustment reduces bias are often untestable or restrictive, this approach may be unreliable in practice.

One approach to addressing unmeasured confounding is to specify and fit the full joint distribution of the treatment, proxy, confounders, and outcome, as in our prior work on hospital admissions [Cochran et al., 2019, Alvarez Avendaño et al., 2020, 2022, 2025]. A notable example of this strategy is the Causal Effect Variational Autoencoder (CEVAE), which uses advances in machine learning [Louizos et al., 2017]. In particular, CEVAE flexibly models the means and variances of Gaussian latent variables using neural networks, allowing for expressive, data-driven modeling of complex relationships. CEVAE, however, does not consider measured confounders and, like many machine learning approaches, may struggle with limited sample sizes. And while VAEs can be expressive, Louizos et al. [2017] note that we currently lack theory to justify when the true model can be identified. In high stakes fields like healthcare, this uncertainty may discourage practitioners from adopting this approach.

In the field of causal inference, there has been a surge of development in proximal causal inference. There are three types of proxies: proxies that are common causes of the treatment and outcome, proxies that causally effect the treatment, and proxies that causally effect the outcome [Cui et al., 2023]. The second and third types are also known as negative control exposure (NCE) and negative control outcome (NCO) respectively [Tchetgen Tchetgen, 2013]. When proxies can be correctly identified and categorized, they can be used to great effect. Kuroki and Pearl introduced the terminology of proxy variables and used two proxies independent from both the outcome and treatment, conditional on the latent variable [Kuroki and Pearl, 2014]. Two invertibility conditions and a restriction to categorical variables ensured strong enough relationships between the variables to recover the ATE.

In a generalization of Kuroki and Pearl’s proof for linear models, Miao et al. achieved identification of the ATE with an NCO and an NCE, for both continuous and discrete variables [Miao et al., 2018]. Their model is shown in Figure 1B. Here V is the NCE, and W is the NCO. One proxy is used to recover the ratio of the relationship between the outcome and the latent variable and between the other proxy and the latent variable, and the other proxy is used to re-scale the associations appropriately [Shi et al., 2020]. This relies on correct identification of proxy types and a “bridge function” that solves an integral equation to achieve identification. When proxies can be correctly categorized into NCEs and NCOs, and the bridge function equation can be solved, this technique is powerful.

One possibility for solving the bridge function equation is through *proximal g-computation* [Tchetgen et al., 2020]. This method selects a parametric model for the bridge function that acts as a form of regularization to stabilize estimation. This is particularly important, because even small errors in estimating $\mathbb{E}[Y|A, V]$ can lead to “excessive uncertainty in obtaining a solution to the equation” [Tchetgen et al., 2020]. However, these models may lack closed form solutions or may require computational techniques like Monte Carlo approximation to solve. The bridge function can also be modified to a form more similar to inverse probability weighting for semiparametric inference with a doubly-robust estimator [Cui et al., 2023]. While they successfully propose a locally efficient estimator, they note that the increased difficulty of implementation may not be worth it.

Other estimation techniques involving two proxies (an NCE and an NCO) include a multiply robust estimator when U, W, V are all binary [Shi et al., 2019]. Additionally, nonparametric identification theory has been summarized neatly in the proximal identification algorithm [Shpitser et al., 2023], which integrates prior theories of proximal causal inference into the world of graphical causal models. In doing so, Shpitser et al. [2023] also introduce a generalization of the front-door criterion for proxy variable settings.

Proxy-based causal inference has powerful theoretical foundations, yet its practical implementation, while possible [Kallus et al., 2022, Sverdrup and Cui, 2023], remains limited. To the best of our knowledge, these techniques have not been adopted beyond methodological papers with simulated data or existing data sets [Cui et al., 2023, Kallus et al., 2022, Miao et al., 2020, Shi et al., 2019, Shpitser et al., 2023, Sverdrup and Cui, 2023, Tchetgen et al., 2020]. A cohort study in non-small cell lung cancer wanted to use proximal causal inference but to achieve sufficient generality for application, “these methods require complicated

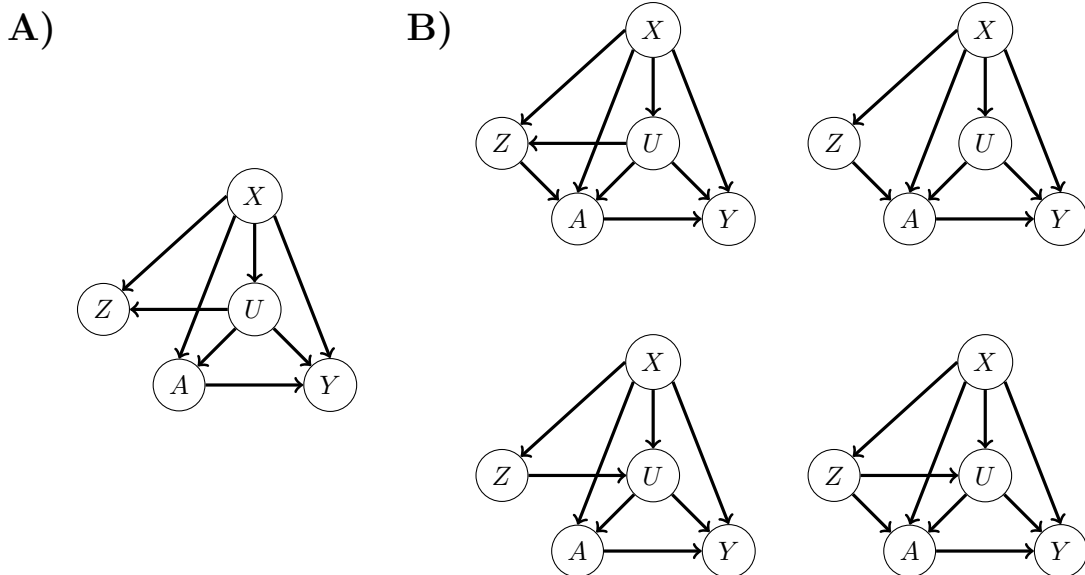


Figure 2: DAGs describing unmeasured confounding: A) with a general proxy variable, B) with alternative causal models that satisfy Corollary 4.1.

estimation procedures that require large sample sizes, which makes these methods unsuitable for many medical applications” [van Amsterdam et al., 2022]. This, combined with the need to separate proxies into NCEs and NCOs, provides motivation for proxy-based approaches that are practical and easy to implement. To bridge this gap, we propose a practical alternative that combines factor analysis with proxy-based causal inference. Factor analysis already has precedence and familiarity among medical researchers [Gagnon-Bartsch and Speed, 2012, Jacob et al., 2016, Wang et al., 2017]. This familiarity supports adoption in practice, while avoiding the issues with categorizing proxies that can serve as both NCOs and NCEs.

3 Causal Framework

We consider the following random variables: measured confounders $X \in \mathbb{R}^l$; unmeasured confounders $U \in \mathbb{R}^k$; proxy variables $Z \in \mathbb{R}^p$; treatment assignment $A \in \mathcal{A}$, typically with $\mathcal{A} = \mathbb{R}_{\geq 0}$ or $\mathcal{A} = \{0, 1\}$; and an outcome $Y \in \mathbb{R}$. These variables capture events related to a patient’s visit to a healthcare provider: Each patient visit has some measured confounders X (like age or sex) along with unmeasured confounders U , such as their needs for treatment and monitoring. The provider collects observations Z of the patient’s health, such as their acuity level or imaging results. Here, Z is assumed to carry imperfect information about U so that Z acts as a proxy for U . Importantly, Z contains only the observations that will eventually be available in EHR. After collecting information about the patient, including the information not recorded in Z , the provider assigns treatment A . Possible treatments include a medication dosage or an admission into the hospital. It is assumed that U can be defined so that the treatment assignment depends on Z only via its relation to the latent variable U . After treatment is assigned, the patient is followed up for some time period, and an outcome Y such as an adverse health event is observed.

We embed these variables into a non-parametric structural equation model (NPSEM) that consists of independent random noises $\{\varepsilon_X, \varepsilon_U, \varepsilon_Z, \varepsilon_A, \varepsilon_Y\}$ and deterministic “assignment” functions $\{f_X, f_U, f_Z, f_A, f_Y\}$ such that our random variables are assigned iteratively:

$$\begin{aligned}
 X &:= f_X(\varepsilon_X), & U &:= f_U(X, \varepsilon_U), & Z &:= f_Z(X, U, \varepsilon_Z), \\
 A &:= f_A(X, U, \varepsilon_A); & Y &:= f_Y(X, A, U, \varepsilon_Y).
 \end{aligned}$$

One practical benefit of NPSEMs is their independence assumptions can be represented concisely in a DAG; each node is a variable and a directed edge exists from one variable to another if the former is an argument in the assignment of the latter. This NPSEM results in Figure 2A. We later relax these generation assumptions.

Our NPSEM defines potential outcomes, following the single world intervention graph (SWIG) framework introduced by Richardson and Robins [2013]. This framework offers us the versatility of potential outcomes as described by Neyman [1923] and Rubin [1974], with the precision and graphical aids of do-calculus described by Pearl et al. [2016]. The idea is to replace the observed intervention A with the fixed intervention $a \in \mathcal{A}$ in all subsequent assignments. This procedure allows us to iteratively define a new set of variables:

$$\begin{aligned} X(a) &:= f_X(\varepsilon_X), & U(a) &:= f_U(X(a), \varepsilon_U), & Z(a) &:= f_Z(X(a), U(a), \varepsilon_Z), \\ A(a) &:= f_A(X(a), U(a), \varepsilon_A); & Y(a) &:= f_Y(X(a), a, U(a), \varepsilon_Y). \end{aligned}$$

The notation “ (a) ” serves to mark that these new variables result from fixing a may not be the originally observed variables. Our assumptions allow us to immediately recover the relations: $X(a) = X$, $U(a) = U$, $Z(a) = Z$, and $A(a) = A$. In the SWIG framework, these relations follow from the principle of causal irrelevance [Richardson and Robins, 2013]. Accordingly, we drop “ (a) ” for variables other than $Y(a)$ from subsequent exposition.

4 Identification

With the potential outcomes defined, our goal is to use the observed variables to estimate the conditional average treatment effect (CATE): $\beta(Z, X) := \mathbb{E}[Y(a_1) - Y(a_0)|Z, X]$ for $a_1, a_0 \in \mathcal{A}$. The CATE tells us the expected difference in outcome if someone with Z and X is given treatment a_1 instead of treatment a_0 . By conditioning on Z and X , we are able to gauge the effect of the intervention on a specific group with Z and X , instead of in the population as a whole. This is particularly useful in applications where treatment effects may vary across subgroups. Estimating the the CATE allows for more targeted inference.

Learning about the CATE is challenging because we only observe what occurs when a patient is assigned to one treatment. We cannot directly estimate the CATE without further manipulation. Identification is the process by which we re-express our causal identity of interest, in our case the CATE $\beta(Z, X)$, in terms of the observed data.

To motivate our identification strategy, it is useful to appreciate how a strategy that ignores the latent variable can go wrong. For simplicity, let $\mathcal{A} = \{0, 1\}$ and omit X . Imagine we wrongly assume the treatment assignment A and outcome Y are influenced directly by proxies Z rather than U . We would then identify the CATE with the expression:

$$\mathbb{E}[Y|Z, A = 1] - \mathbb{E}[Y|Z, A = 0],$$

i.e. subtracting the mean outcome for people who did not receive treatment from the mean outcome for people who did receive treatment with the same characteristics Z .

To see how this approach can fail, suppose instead that the true data-generating process follows our NPSEM and that Y is generated via a simple additive noise model:

$$f_Y(a, u, \varepsilon_Y) = \varepsilon_Y + g_0(u) + ag_1(u),$$

where g_0 and g_1 are arbitrary functions of the latent variable U , and $\mathbb{E}[\varepsilon_Y] = 0$. The only additional assumption here is the additivity of noise. In this case, the individual treatment effect is $Y(1) - Y(0) = g_1(U)$, so the true CATE is: $\mathbb{E}[g_1(U)|Z]$.

Now consider what the expression $\mathbb{E}[Y|Z, A = 1] - \mathbb{E}[Y|Z, A = 0]$ actually estimates under this model. It differs from the true CATE, $\mathbb{E}[g_1(U)|Z]$, and instead equals:

$$\mathbb{E}[g_1(U)|Z, A = 1] + (\mathbb{E}[g_0(U)|Z, A = 1] - \mathbb{E}[g_0(U)|Z, A = 0]).$$

The bias can be written compactly as:

$$\mathbb{E}[h(U, Z)|Z, A = 1] - \mathbb{E}[h(U, Z)|Z, A = 0],$$

where $h(U, Z) = g_0(U) + \mathbb{P}(A = 0|Z)g_1(U)$. In general, this bias does not vanish, except under special conditions, e.g $h(U, Z) \perp\!\!\!\perp A | Z$.

To better understand when adjusting for proxies introduces bias, suppose the outcome model is affine in the unobserved variable U . Specifically, let

$$g_0(u) = c_0 + c_1' u; \quad g_1(u) = c_2 + c_3' u.$$

so the effect of U on Y enters through linear terms. Under this assumption, the bias that arises from adjusting on Z simplifies to:

$$(c_1 + \mathbb{P}(A = 0|Z)c_3)' (\mathbb{E}[U|Z, A = 1] - \mathbb{E}[U|Z, A = 0]).$$

This expression highlights two key drivers of bias: (1) how much U affects the outcome, and (2) how imbalanced U is between treated and untreated individuals with the same value of Z . The bias is zero exactly when $c_1 + \mathbb{P}(A = 0|Z)c_3$ and $\mathbb{E}[U|Z, A = 1] - \mathbb{E}[U|Z, A = 0]$ are orthogonal—roughly speaking, when the direction in which U affects the outcome is perpendicular to the direction in which U is imbalanced across treatment groups. In particular, bias is small if either U has little or no effect on the outcome (c_1 and c_3 are small), or the treatment assignment does not tell you anything more about U beyond what is already captured in Z ($\mathbb{E}[U|Z, A = 1] - \mathbb{E}[U|Z, A = 0]$ is small). Put simply, the bias will be small when the amount of confounding between A and Y that comes from U is small, either because U has little effect on the outcome, or its influence is well-approximated by Z .

4.1 A general strategy for identification

As we saw, simply adjusting for the proxy variable Z does not recover the CATE, so an alternative identification strategy is needed. We begin by outlining the most general version of the strategy, before turning to the practical implementation we use. We rely on two general assumptions. First, although U is unobserved, we assume that the observed variables contain enough information to recover certain functions of U in expectation. Formally:

Assumption 4.1. There is a vector-valued function $g(U, X)$ so that $\mathbb{E}[g(U, X)|Z, A, X]$ can be identified from the observed variables (Z, A, X) .

Second, we require these functions are expressive enough to capture how the expected potential outcomes vary with treatment and covariates. This is essentially a working model for the potential outcome. That is:

Assumption 4.2. The causal quantity $\mathbb{E}[Y(a)|U, X]$ can be written as $\tau(a, X)'g(U, X)$ for some vector-valued function $\tau(a, X)$ and each $a \in \mathcal{A}$.

Combined, these assumptions provide a general strategy for identification:

Theorem 4.1. Assume Assumptions 4.1–4.2 hold with vector-valued functions τ and g defined therein. Then as long as $\tau(A, X)$ is the unique solution to:

$$\mathbb{E}[Y|Z, A, X] = \tau(A, X)' \mathbb{E}[g(U, X)|Z, A, X],$$

we can identify the CATE by way of

$$\beta(Z, X) = (\tau(a_1, X) - \tau(a_0, X))' \mathbb{E}[g(U, X)|Z, X].$$

We include the proof in Appendix A. This theorem outlines a two-step strategy for identifying the CATE. The first step is to target a lower-dimensional summary of U , captured by the conditional expectation $\mathbb{E}[g(U, X)|Z, A, X]$. This quantity is both a function of the observed variables and can be recovered from them. Once we have this quantity, we treat it as a predictor and use it to model the conditional mean of the outcome Y by learning the function $\tau(A, X)$ in the expression $\mathbb{E}[Y|Z, A, X] = \tau(A, X)' \mathbb{E}[g(U, X)|Z, A, X]$. This is done using regression. With $\tau(A, X)$ recovered, we then compute the CATE.

We can relax the generating assumptions, allowing for greater flexibility in underlying models, including the possibility of Z directly influencing A or A directly influencing Z :

Corollary 4.1. Suppose Assumptions 4.1–4.2 hold, and the NPSEM corresponds to one of the DAGs in Figure 2B, with potential outcomes defined accordingly. Then the conclusions of Theorem 4.1 hold.

Each NPSEM in Figure 2B, together with its associated potential outcomes, implies the independence relations: $Y(a) \perp\!\!\!\perp Z \mid U, X$ and $Y(a) \perp\!\!\!\perp A \mid U, X$. These independence conditions are used to establish conclusions analogous to those in Theorem 4.1 across all the depicted causal structures. This shows that our strategy can tolerate ambiguity in structural assumptions, which is often unavoidable in practice. Even if we cannot determine which NPSEM generated the data, identification still holds as long as one of the models in Figure 2B is valid. This is especially relevant in applied settings, where a variable assumed to be a proxy might instead be a direct cause of U , or an instrument. Our strategy accommodates these distinctions without requiring precise knowledge of each variable’s structural role, making it useful when such details are difficult to verify.

4.2 A specific, parametric strategy for identification

Our ability to gather information about the latent variable (Assumption 4.1) forms the cornerstone of our identification strategy. Here, we outline how to identify expectations of the form $\mathbb{E}[g(U, X) \mid Z, A, X]$ by imposing stronger assumptions on the variables U , Z , A , and X . Notably, the outcome Y is not included in these assumptions. Our task later will be to show that our final estimate of the CATE is relatively insensitive to these additional assumptions. We consider the multiple indicators multiple causes (MIMIC) model [Tekwe et al., 2014, Chang et al., 2020], an extension of factor analysis that incorporates covariates:

Assumption 4.3. Assume the following parametric model: First, ε_X , ε_U , ε_Z , and ε_A are all independent multivariate standard normals. Second, assignment functions are given by:

$$\begin{aligned} f_X(\varepsilon_X) &= \varepsilon_X \Theta^{1/2} & f_U(\varepsilon_U) &= \Gamma X + \varepsilon_U, \\ f_Z(U, \varepsilon_Z) &= \Lambda U + \nu + \Psi^{1/2} \varepsilon_Z; & f_A(U, \varepsilon_A) &= b'U + c + \varepsilon_A, \end{aligned}$$

where $\Psi \in \mathbb{R}^{p \times p}$ is diagonal and positive definite; $\Lambda \in \mathbb{R}^{p \times k}$ and $\Gamma \in \mathbb{R}^{k \times m}$ are full rank; and $\nu \in \mathbb{R}^p$, $c \in \mathbb{R}$, and $b \in \mathbb{R}^k$, with $k < p$.

As discussed in Tekwe et al. [2014], Chang et al. [2020], parametric models of this form identify the parameters only up to an orthogonal transformation of the latent factor U . In applied settings, this indeterminacy is typically resolved by imposing a constraint or applying a rotation post hoc to select among models with equivalent likelihoods. For simplicity, we adopt a standard identifying constraint from the factor analysis literature (though other constraints would serve equally well in what follows):

Assumption 4.4. Loading matrix Λ is lower triangular with positive diagonal entries.

Under this constraint, we now establish a result on identifiability:

Lemma 4.1. Given Assumptions 4.3 and 4.4, $\mathbb{E}[g(U, X) \mid Z, A, X]$ can be identified from the observed variables Z , A , and X for any vector-valued function g .

This lemma implies that Assumption 4.1 is satisfied. Note also that Assumption 4.2 is trivially satisfied, since this lemma puts no restrictions on what functions g can be used to capture $\mathbb{E}[Y(a) \mid U, X]$. Therefore, the CATE can be identified as described above:

Corollary 4.2. Suppose the potential outcomes are defined, and Assumptions 4.3, and 4.4 hold. We can identify the CATE using the procedure outlined in Theorem 4.1.

5 Estimation

We use our identification strategy to guide the steps of estimation in practice. We walk through a concrete example that reflects how an applied investigator would typically approach this problem in practice, and later describe how to estimate effects in other settings.

The applied investigator would first identify the roles of the variables at hand: the treatment A , outcome Y , measured confounders or covariates X , proxy variables Z , and possible unmeasured confounders U .

The investigator would then specify a working model for the potential outcome in terms of unmeasured confounders U , treatment A , and covariates X . For simplicity, we choose the following working model:

$$\mathbb{E}[Y(a)|X, U] = \nu_0 + \nu_1'U + \nu_2'UA + \nu_3A.$$

This model can be factored as $(\alpha + \gamma A)' [1 \quad U]'$ for an appropriate choice of α and γ . This allows us to see that this model corresponds to $g(U, X) = [1 \quad U]'$ and $\tau(a, X) = \alpha' + \gamma'A$ in the earlier identification proof. We also assume a MIMIC model for (U, Z, A, X) (Assumption 4.3). Importantly, our choice of working model allows for closed-form expressions of the conditional means required in the outcome model, enabling efficient computation. When such expressions are not available (e.g., under more complex or nonlinear models), these quantities can be computed using Monte Carlo integration.

Once the working model is specified, we fit the MIMIC model to our observations of X , A , and Z . Existing latent modeling packages like *lavaan* in R or MPlus can fit the MIMIC model, making this step accessible to applied researchers. Since this requires selecting the number of factors, we fit models with 1 to p factors and select via the lowest Akaike information criterion (AIC) value. Subsequently, we use the fitted model to estimate two quantities, $\mathbb{E}[U|Z, A, X]$ and $\mathbb{E}[U|Z, X]$, for each patient at their observed values of Z , A , and X . Let $\hat{\mathbb{E}}[U|Z, A, X]$ and $\hat{\mathbb{E}}[U|Z, X]$ denote the estimated values. See Appendix B for the derivation of a closed form for $\mathbb{E}[U|Z, A, X]$ and $\mathbb{E}[U|Z, X]$.

We then estimate the parameters of the potential outcome model, ν_0 , ν_1 , ν_2 , and ν_3 , by fitting a linear regression of the outcome Y on the observed variables Z , A , and X . Under our assumptions, this model takes the form

$$\mathbb{E}[Y|Z, A, X] = \nu_0 + \nu_1'\mathbb{E}[U|Z, A, X] + \nu_2'\mathbb{E}[U|Z, A, X]A + \nu_3A,$$

where the regression coefficients correspond directly to those in the potential outcome model. Since U is unobserved, we substitute in its estimate, $\hat{\mathbb{E}}[U|Z, A, X]$, obtained from the fitted MIMIC model. The resulting model includes two main effects and one interaction.

Upon performing linear regression, we recover estimates of the parameters of the potential outcome model, which we denote by $\hat{\nu}_0$, $\hat{\nu}_1$, $\hat{\nu}_2$, and $\hat{\nu}_3$. We put together these estimates and our estimate of $\hat{\mathbb{E}}[U|Z, X]$ to arrive at the CATE estimate:

$$\begin{aligned} \hat{\beta}(X, Z) &= (\hat{\nu}_0 + \hat{\nu}_1'\hat{\mathbb{E}}[U|Z, X] + \hat{\nu}_2'\hat{\mathbb{E}}[U|Z, X]a_1 + \hat{\nu}_3a_1) \\ &\quad - (\hat{\nu}_0 + \hat{\nu}_1'\mathbb{E}[U|Z, X] + \hat{\nu}_2'\mathbb{E}[U|Z, X]a_0 + \nu_3a_0) \\ &= (a_1 - a_0)(\hat{\nu}_2'\hat{\mathbb{E}}[U|Z, X] + \hat{\nu}_3). \end{aligned}$$

The entire estimation procedure can be formalized using estimating equations, with consistency and asymptotic normality provable under standard conditions. However, we omit these derivations here, as they are unlikely to be of practical concern for applied investigators.

6 Simulation

We evaluate our method using simulated data where the true treatment effect is known. We examine bias, variance, and asymptotic behavior. When the latent variable model is correctly specified, we also consider the ratio of proxies to latent confounders (p/k). To assess robustness to model misspecification, we consider scenarios where the mean function is quadratic in U but modeled as linear, where U follows a skew normal rather than a normal distribution, and where the treatment A is binary rather than continuous. Finally, we explore robustness to violations of structural assumptions, including cases where Z is a direct confounder or an IV, but is treated as a proxy. All computations are completed using the parametric strategy from Section 5, with $g(U, X) = [1, U]'$.

We compare our method to inverse probability weighting (IPW), linear models, an IV approach, and proximal causal inference. See Appendix C for details. Briefly, IPW uses a linear regression model for A in terms of Z to determine the weights and then models Y with a linear model in A [Naimi et al., 2014]. For binary treatments, the linear model for A is replaced with a logistic regression. The linear method uses a linear regression model for Y in terms of A and Z . For the proximal method, we randomly split the proxy variables evenly into NCOs and NCEs. Since the proxies are interchangeable, this is equivalent to

averaging over all possible even divisions into NCOs and NCEs. Since most of these techniques estimate the Average Treatment Effect (ATE) $\mathbb{E}[Y(1) - Y(0)]$, rather than the CATE, we take the expectation of our CATE estimations since $\mathbb{E}[\mathbb{E}[Y(1) - Y(0)|Z]] = \mathbb{E}[Y(1) - Y(0)]$.

We use the data-generating process described in Assumption 4.3 as the baseline. The outcome is generated as $Y = (\alpha + A\gamma)[1 \ U]'$, where α and γ are selected to yield a true average treatment effect (ATE) of 0.3. Measured confounders X are ignored. For each setting, we generate 1000 independent samples and apply each method to estimate the treatment effect. This process is repeated across 1000 simulation replicates. Then, for each robustness check, we slightly modify this process in targeted ways to test how well the method performs under deviations from the ideal case. We follow Tucker et al. [1969], Nieser and Cochran [2023] to generate realistic loading and diagonal covariance matrices with varying levels of communality. We also vary the sample size, the number of proxies (p), the number of latent dimensions (k), and the strength of confounding. To evaluate our method’s coverage, we construct 95% bootstrap confidence intervals. Source code can be found at <https://github.com/HaleyColgateKottler/LatentProxyVars>, and details in Appendix C. Since the IV method is sensitive to assumption violations, it is excluded from the main plots for readability. For results including IV as a comparator, see Appendix C.

Figure 3A illustrates estimation accuracy across varying sample sizes. As the sample size increases, the 25th and 75th percentiles for our method’s estimates tighten around the true effect value of 0.30, suggesting consistency. At smaller sample sizes, our estimates show greater accuracy than the comparison techniques.

Figure 3B shows our method is more accurate with larger ratios of proxies to latent confounders (p/k). Accuracy improves notably when this ratio increases from 1 to 2 and from 2 to 3, indicating that having three proxies per latent dimension is particularly beneficial. This aligns with expectations, as factor analysis models typically require at least three observed variables per latent factor. With at least three proxies per dimension, our method outperforms all comparison methods in terms of how close the median is to the true effect, until the proximal causal inference method catches up around a p/k ratio of 8.

For a sample size of 500, bootstrap confidence intervals give a coverage of 96%, using 2000 resamples and 150 simulation replications. Since bootstrapping accounts for variability from both modeling steps, and is generally conservative, this is a reasonable coverage estimate.

Figure 4A demonstrates the ability of our method to maintain accurate estimates despite an incorrect mean-model. In this scenario, we assume for estimation that $\mathbb{E}[Y(a)|U] = [1 \ U] \tau(a, X)$, which can be seen as a first moment approximation, but generate data with $\mathbb{E}[Y(a)|U] = [1 \ U \ U^2] \tau(a, X)$ instead. We see that with this adjustment in data generation, all the comparison methods are biased, while our estimate remains unbiased.

Our approach is robust even when the distribution of the latent variable is misspecified (Figure 4B). In this scenario, the data is generated with a skew normal distribution for U , even though our method assumes a normal distribution. Our method exhibits lower bias than all comparison methods except proximal causal inference, and its estimates have substantially lower variance than those from proximal causal inference. As a result, it achieves the highest overall estimation accuracy.

Figure 4C illustrates the robustness of our method when applied to binary treatments. We generate a binary intervention using a probit model, $A^* = \mathbb{I}_{A \geq 0}$, but continue to assume a continuous treatment during estimation. All methods exhibit some bias under this mismatch, though our method and proximal causal inference are notably less biased than the others. However, proximal causal inference produces estimates with higher variance, resulting in lower overall accuracy. Our method offers the best bias–variance tradeoff.

Our method is also robust to violations in structural assumptions (Figure 4D). In Section 4, we showed how treating a proxy as a direct confounder introduces bias. Here we consider the opposite: Z is a direct confounder, not a proxy. As expected, linear and IPW techniques—which correctly treat Z as a confounder—are less biased than ours. Nevertheless, our method still recovers the correct sign and order of magnitude. So even when a confounder is incorrectly assumed to be a proxy variable, our method can produce reasonable results.

Figure 4E explores the impact of treating an IV as a proxy. We apply our technique to data where Z and U are independent multivariate normal random variables, and generate A via $A = b_1'U + b_2'Z + c + \varepsilon_A$, with $\varepsilon_A \sim \mathcal{N}(0, 1)$. In this setting, our method, like proximal causal inference, exhibits slight bias but is less biased than linear regression and IPW. Variance is comparable to both IV and proximal, though larger than that of linear and IPW. IV is the only method that yields an unbiased estimate (Appendix C), as expected. These results suggest that our method remains relatively robust even when IVs are mistaken for proxies.

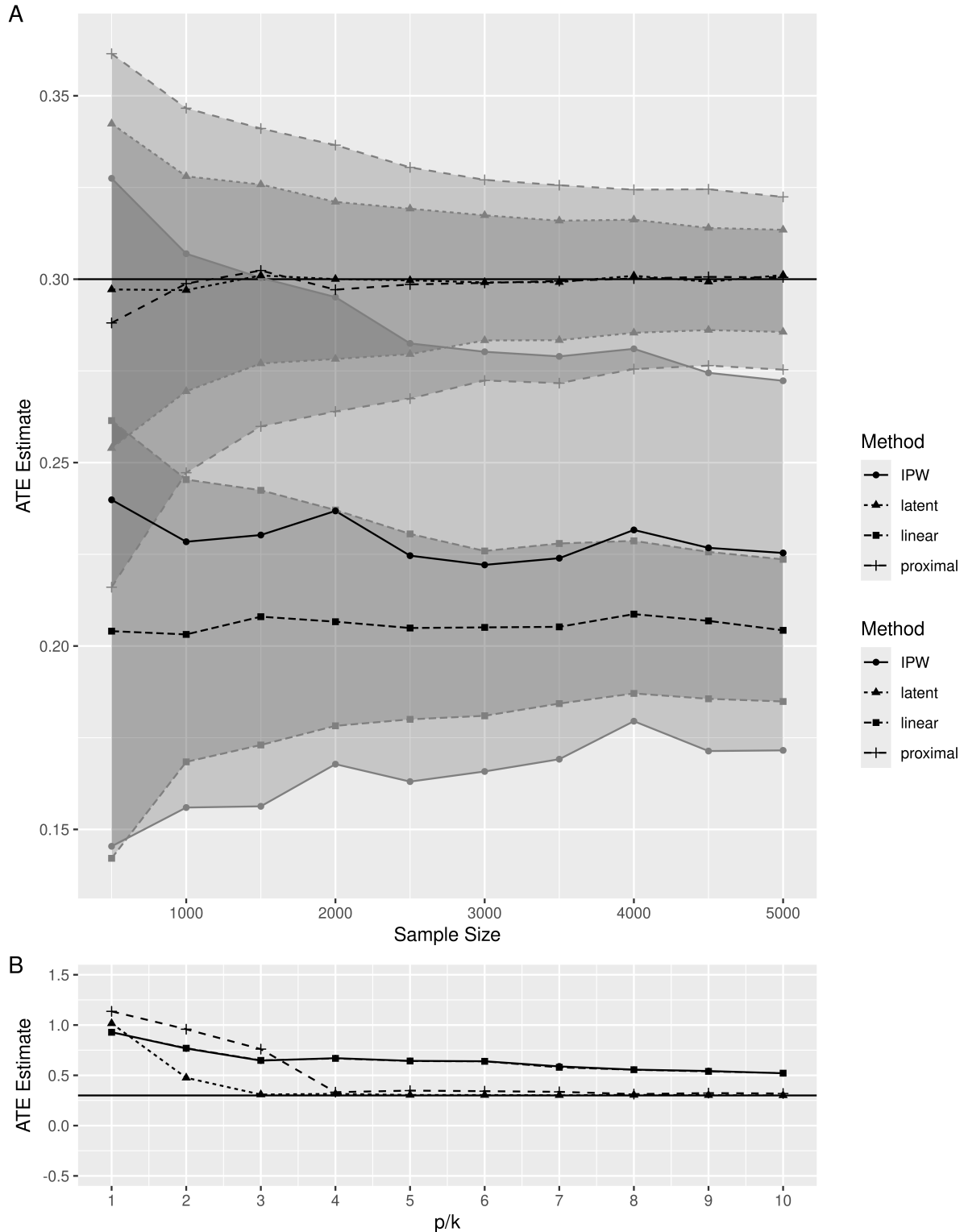


Figure 3: A) Estimation accuracy of our method and comparison methods as a function of sample size, reported as the median estimate and interquartile ranges (25th and 75th percentiles) across simulation replications. B) Estimation accuracy as function of different ratios of proxies to latent confounders (p/k), reported as the median estimate across simulation replications. Our method is the most accurate for all sample sizes, rivaled only by proximal causal inference which has a higher mean squared error. With $p/k \geq 2$ our method is more accurate than the comparison methods, though with higher p/k ratios, proximal causal inference obtains similar accuracy.

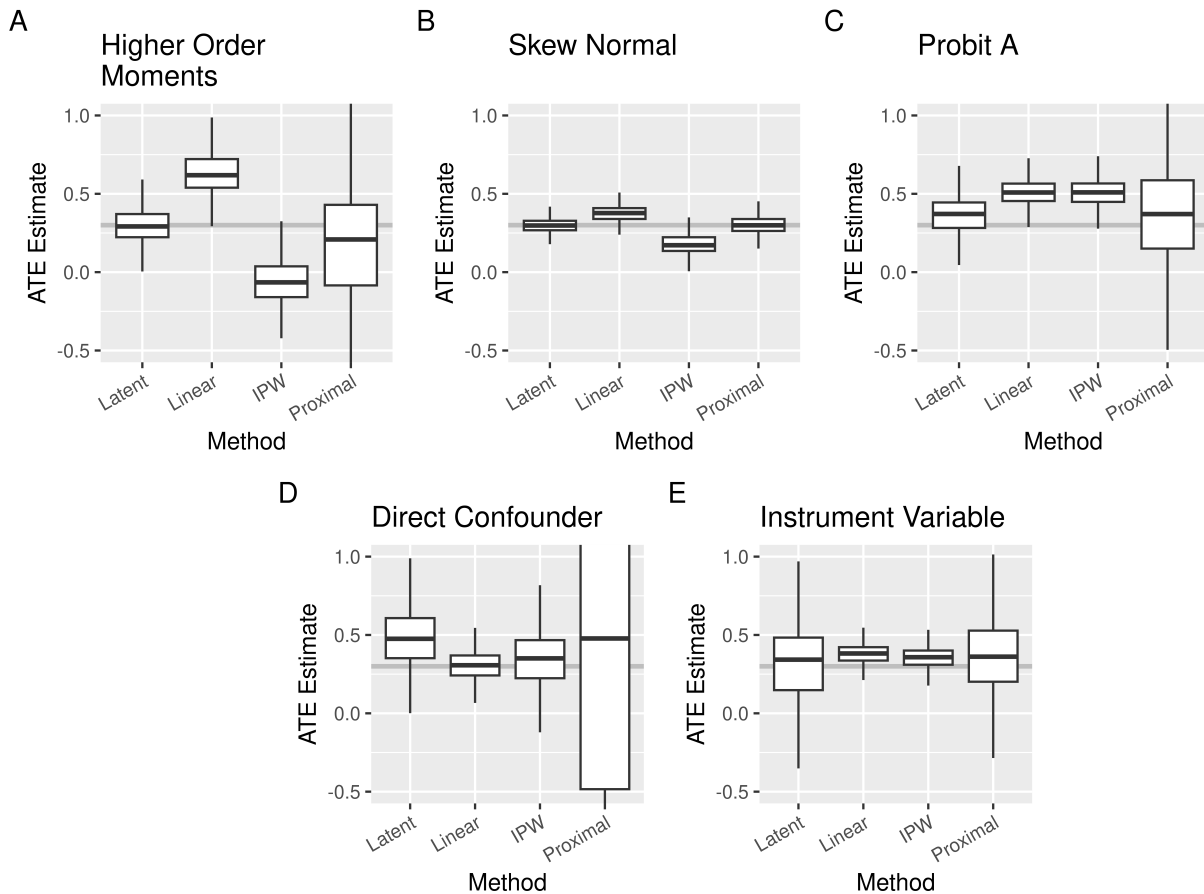


Figure 4: Performance of methods under different modeling and structural assumptions: A) the true outcome generation process is quadratic in U but the estimator is linear, B) the latent variable is skew normal instead of normal, C) the treatment is binary but estimated as continuous, D) Z is a confounder not a proxy, E) Z is an instrument not a proxy. The centerline is the median, the hinges show the inter-quartile range (IQR), and the whiskers show the minimum of the highest estimate or 1.5IQR from the upper hinge and the maximum of the lowest estimate or 1.5IQR from the lower hinge.

For the cases when the model is incorrect, we computed our method’s coverage using 100 replications with 500 bootstrap replications. We achieve a coverage of 0.96 for the higher order outcome generation, 0.94 for the skew normal latent variable, 0.87 for the binary treatment, 0.97 for the direct confounder treated as a proxy, and 0.94 for the IV treated as a proxy. The coverage is slightly lower in the binary case, but otherwise similar to the coverage when the model is correctly specified.

7 Case Study

We applied our method to investigate the impact of hospitalization or discharge on older adults in the ED with chest pain. Older adults (65+ years) frequently present to EDs with chest pain, a nonspecific symptom that complicates decisions regarding whether they should be admitted or discharged [Alvarez Avendaño et al., 2020]. This decision is clinically significant because hospital admission poses risks for older adults, such as deconditioning and hospital-acquired infections, but chest pain can also be indicative of serious conditions so not admitting a patient also poses risks.

Our analysis uses EHR data from MIMIC-IV v2.2, a large, de-identified database containing real hospital records from a tertiary medical center in Boston, Massachusetts [Johnson et al., 2020]. We restricted the dataset to patients aged 65 or older who presented to the ED with “chest pain” listed in their chief complaint and were assigned an acuity level of 2 or 3 since those are the patients for whom the decision to admit or discharge is unclear. We excluded records where the disposition was neither admission nor discharge. Table 1 provides an overview of the data, including specific lists of covariates and proxies. Disposition is our treatment, and readmission or mortality within 30 days of discharge from any unit (ED or inpatient) is our outcome of interest. We treat demographic data as covariates. Data gathered during triage, along with total treatment time, are treated as proxies.

We handled missing data in several ways. First, we excluded any records missing the treatment or outcome, or missing three or more variables out of the proxies or covariates. We introduced an “Unknown” category for insurance type, marital status, and race to account for possible differences in patients without full demographic data. Finally, we applied multiple imputation once using the MICE R package [van Buuren and Groothuis-Oudshoorn, 2011] including all variables. This resulted in a final dataset of 7081 ED visits. For categorical variables, we treat the most common level as the reference class. To incorporate covariates, we adopted the MIMIC model as described in Section 4.2. For clarity, we use MIMIC-IV to refer to the data set and MIMIC to refer to the multiple indicators multiple causes model. Details of this model are provided in Appendix B.

For comparison, we used the same comparison methods described in the prior section, in addition to an unadjusted estimate. Since the proxies are not interchangeable, we tested every possible even split of the proxies into NCOs and NCEs for proximal causal inference. Confidence intervals (CIs) for all estimates were computed using 5000 bootstrap replications.

A direct comparison of patients admitted to the hospital versus those discharged home, without adjusting for other covariates, estimated the ATE as 0.113 [0.097, 0.130], suggesting that hospital admission increases the risk of 30-day readmission for the average patient. IPW produced a much larger and more variable, estimate of 0.648 [-0.336, 1.637]. A basic linear model provided a smaller estimate of 0.074 [0.052, 0.095]. Proximal causal inference resulted in a range of estimates from 0.044 to 0.172, with a median value of 0.089. The latent variable method yielded a distinctly different result: a numerically negative estimate of -0.021 [-0.192, 0.109]. This estimate suggests that hospitalization may reduce the risk of readmission for the average patient, in contrast to the positive estimates from the other methods.

8 Conclusion

We presented a practical method for using proxy variables in causal inference that avoids the technical challenges of existing approaches. We use a factor analysis model to relate proxies and treatment to latent confounders, building covariates which feed into the outcome model that adjusts for unmeasured confounding. Our simulations demonstrated several key insights. First, categorizing proxies as confounders leads to biased estimates, underscoring the need for dedicated proxy methods. Our approach significantly reduces this bias,

Table 1: Demographics, triage data, and outcome by disposition

		Admitted	Home	Overall
Covariates	N (% present)	Mean (SD)	Mean (SD)	Mean (SD)
Age	7081 (100)	75.4 (7.5)	73.8 (7.1)	74.7 (7.4)
	Level	Count (%)	Count (%)	Count (%)
Gender	Female	1930 (48.0)	1798 (58.8)	3728 (52.6)
	Male	2093 (52.0)	1260 (41.2)	3353 (47.4)
Race/Ethnicity	American Indian/ Alaska Native	6 (0.1)	5 (0.2)	11 (0.2)
	Asian	155 (3.9)	124 (4.1)	279 (3.9)
	Black	632 (15.7)	623 (20.4)	1255 (17.7)
	Hispanic/Latinx	227 (5.6)	249 (8.1)	476 (6.7)
	Other	181 (4.5)	172 (5.6)	353 (5.0)
	White	2787 (69.3)	1881 (61.5)	4668 (65.9)
	Missing	35 (0.9)	4 (0.1)	39 (0.6)
Insurance	Medicaid	100 (2.5)	42 (1.4)	142 (2.0)
	Medicare	2545 (63.3)	918 (30.0)	3463 (48.9)
	Other	1341 (33.3)	517 (16.9)	1858 (26.2)
	Missing	37 (0.9)	1581 (51.7)	1618 (22.8)
Marital status	Divorced	347 (8.6)	127 (4.2)	474 (6.7)
	Married	1846 (45.9)	687 (22.5)	2533 (35.8)
	Single	684 (17.0)	323 (10.6)	1007 (14.2)
	Widowed	1073 (26.7)	332 (10.9)	1405 (19.8)
	Missing	73 (1.8)	1589 (52.0)	1662 (23.5)
Proxies	N (% present)	Mean (SD)	Mean (SD)	Mean (SD)
Heart rate	7073 (99.9)	79.2 (17.4)	76.3 (14.7)	78.0 (16.4)
Systolic blood pressure	7069 (99.8)	140.6 (25.4)	146.8 (23.1)	143.3 (24.6)
Diastolic blood pressure	7060 (99.7)	73.5 (15.3)	75.7 (14.3)	74.5 (14.9)
Respiration rate	7014 (99.1)	18.1 (2.8)	17.6 (1.9)	17.9 (2.5)
O2 saturation	7038 (99.4)	97.6 (3.1)	98.3 (1.7)	97.9 (2.6)
Temperature	6971 (98.4)	98.0 (1.0)	97.9 (0.8)	98.0 (0.9)
Treatment time	7148 (100)	7.1 (4.5)	13.9 (9.0)	10.1 (7.6)
	Level	Count (%)	Count (%)	Count (%)
Acuity	2	3469 (86.2)	2181 (71.3)	5650 (79.8)
	3	554 (13.8)	877 (28.7)	1431 (20.2)
Outcome	Level	Count (%)	Count (%)	Count (%)
30 day readmission	Yes	888 (22.1)	329 (10.8)	1217 (17.2)
	No	3135 (77.9)	2729 (89.2)	5864 (82.8)

maintains lower variance than proximal causal inference, and achieves higher overall accuracy compared to standard linear regression and IPW under correct model specifications.

Moreover, we found our method to be surprisingly robust under various forms of model misspecification. When using a linear model to approximate a quadratic relationship, assuming normality when latent variables are skew-normal, or assuming continuous treatments despite binary treatment generation, our estimates remained accurate and were more reliable than estimates produced by comparator methods. Our method was only outperformed when a direct confounder or an IV was incorrectly treated as a proxy, but even then, only by methods that correctly accounted for these variables as confounders or IVs, as one would expect. Despite that, our method became slightly biased, although estimates retained the correct sign and plausible magnitude.

In our case study involving older adults presenting to the ED for chest pain, our method uniquely estimated a numerically negative ATE of hospitalization on readmission, aligning better with prior literature and clinical expectations [Alvarez Avendaño et al., 2020]. By contrast, comparison methods produced uniformly positive ATE estimates. This difference illustrates how carefully designed proxy variable methods can critically impact clinical interpretations and subsequent recommendations.

Our results highlight the practical limitations of existing proximal causal inference methods [Miao et al., 2018, Tchetgen et al., 2020]. While its theoretical foundation is strong, our simulations and case study suggest that in finite samples, proximal estimates can be highly variable, often more so than other methods. This limits their practical utility, especially when sample sizes are small. A second challenge is the requirement to classify proxies as either NCEs or NCOs. In our case study, we randomly assigned half the proxies to each category. This led to wide variability in estimates, ranging from 0.044 to 0.172, depending solely on the categorization. Our method avoids this sensitivity by treating all proxies the same, reducing the burden on users and improving stability in real-world settings.

We acknowledge several limitations. First, our method cannot handle every possible relationship between the confounders (X, U) and the outcome Y . This limits the expressiveness of our technique, though we did demonstrate that with $g(U, X) = [1, U]'$, we were able to capture accurate ATE estimates even when Y had a quadratic dependence on U . Second, we computed confidence intervals using bootstrapping. This led to overly conservative estimates. Additionally, our method may be biased when we treat a confounder as a proxy, as shown in simulation. While we believe our ATE estimate to be more realistic in the case study, we would need an randomized controlled trial to validate our estimates. A final limitation is that successful applications of our method depends not only on statistical performance but also on practitioner uptake. Whether practitioners eventually adopt the method will depend on how our method is received by the community.

Future work will aim to extend robustness and flexibility, incorporating a broader class of approximations for both the latent variable and its effect on the outcome and exploring analytical methods for confidence interval estimation. A promising direction includes developing automated approaches that accurately distinguish proxies and confounders without explicit user categorization. Ultimately, by providing a practical and robust tool for handling proxies, we hope to encourage broader adoption of proxy-based causal inference methods.

Acknowledgments

Research of Haley Colgate Kottler was supported in part by National Science Foundation Award DMS-2023239 through the Institute for Foundations of Data Science and Haley Colgate Kottler and Amy Cochran were supported in part by the University of Wisconsin Fall Competition.

9 Data availability statement

The data and code underlying the robustness tests described in this article are available at <https://github.com/HaleyColgateKottler/LatentProxyVars>. The code used to analyze the case study is available at <https://github.com/HaleyColgateKottler/CaseStudy>. The case study data is available at <https://mimic.mit.edu/>.

References

- Sebastian A Alvarez Avendaño, Amy L Cochran, Brian Patterson, Manish Shah, Maureen Smith, and Gabriel Zayas-Cabán. The average effect of emergency department admission on readmission and mortality for older adults with chest pain. *Medical Care*, 58(10):881–888, 2020.
- Sebastian A Alvarez Avendaño, Amy L Cochran, Keith E Kocher, Brian W Patterson, and Gabriel Zayas-Cabán. Average response curves for treatment time in the emergency department. *arXiv preprint arXiv:2203.04372*, 2022.
- Sebastian Alejandro Alvarez Avendaño, Amy Cochran, Valerie Odeh Couvertier, Brian Patterson, Manish Shah, and Gabriel Zayas-Cabán. Revisits, readmission, and mortality from emergency department admissions for older adults with vague presentations: Longitudinal observational study. *JMIR aging*, 8(1): e55929, 2025.
- Chi Chang, Joseph Gardiner, Richard Houang, and Yan-Liang Yu. Comparing multiple statistical software for multiple-indicator, multiple-cause modeling: an application of gender disparity in adult cognitive functioning using midus ii dataset. *BMC Medical Research Methodology*, 20:1–14, 2020.
- Amy L. Cochran, Paul J. Rathouz, Keith E. Kocher, and Gabriel Zayas-Cabán. A latent variable approach to potential outcomes for emergency department admission decisions. *Statistics in Medicine*, 38(20):3911–3935, 2019. doi: <https://doi-org.ezproxy.library.wisc.edu/10.1002/sim.8210>. URL <https://onlinelibrary-wiley-com.ezproxy.library.wisc.edu/doi/abs/10.1002/sim.8210>.
- Yifan Cui, Hongming Pu, Xu Shi, Wang Miao, and Eric Tchetgen Tchetgen. Semiparametric proximal causal inference, 2023.
- Johann A Gagnon-Bartsch and Terence P Speed. Using control genes to correct for unwanted variation in microarray data. *Biostatistics*, 13(3):539–552, 2012.
- Sander Greenland. The Effect of Misclassification in the Presence of Covariates. *American Journal of Epidemiology*, 112(4):564–569, 10 1980. ISSN 0002-9262. doi: 10.1093/oxfordjournals.aje.a113025. URL <https://doi.org/10.1093/oxfordjournals.aje.a113025>.
- Laurent Jacob, Johann A Gagnon-Bartsch, and Terence P Speed. Correcting gene expression data when neither the unwanted variation nor the factor of interest are observed. *Biostatistics*, 17(1):16–28, 2016.
- A Johnson, L Bulgarelli, T Pollard, S Horng, LA Celi, and R Mark. Mimic-iv (version 1.0), 2020.
- Nathan Kallus, Xiaojie Mao, and Masatoshi Uehara. Causal inference under unmeasured confounding with negative controls: A minimax learning approach, 2022.
- Manabu Kuroki and Judea Pearl. Measurement bias and effect restoration in causal inference. *Biometrika*, 101(2):423–437, 03 2014. ISSN 0006-3444. doi: 10.1093/biomet/ast066. URL <https://doi.org/10.1093/biomet/ast066>.
- Christos Louizos, Uri Shalit, Joris Mooij, David Sontag, Richard Zemel, and Max Welling. Causal effect inference with deep latent-variable models, 2017. URL <https://arxiv.org/abs/1705.08821>.
- Wang Miao, Zhi Geng, and Eric J Tchetgen Tchetgen. Identifying causal effects with proxy variables of an unmeasured confounder. *Biometrika*, 105(4):987–993, 08 2018. ISSN 0006-3444. doi: 10.1093/biomet/asy038. URL <https://doi.org/10.1093/biomet/asy038>.
- Wang Miao, Xu Shi, and Eric Tchetgen Tchetgen. A confounding bridge approach for double negative control inference on causal effects, 2020.
- Ashley I Naimi, Erica EM Moodie, Nathalie Auger, and Jay S Kaufman. Constructing inverse probability weights for continuous exposures: a comparison of methods. *Epidemiology*, 25(2):292–299, 2014.

- Jerzy S Neyman. On the application of probability theory to agricultural experiments. essay on principles. section 9. *Annals of Agricultural Sciences*, 10:1–51, 1923.
- Kenneth J Nieser and Amy L Cochran. Addressing heterogeneous populations in latent variable settings through robust estimation. *Psychological methods*, 28(1):39, 2023.
- Elizabeth L. Ogburn and Tyler J. VanderWeele. On the nondifferential misclassification of a binary confounder. *Epidemiology*, 23(3):433–439, 2012. ISSN 10443983. URL <http://www.jstor.org/stable/23214273>.
- J. Pearl, M. Glymour, and N.P. Jewell. *Causal Inference in Statistics: A Primer*. Wiley, 2016. ISBN 9781119186847. URL <https://books.google.com/books?id=L3G-CgAAQBAJ>.
- Jose M. Peña, Sourabh Balgi, Arvid Sjölander, and Erin E. Gabriel. On the bias of adjusting for a non-differentially mismeasured discrete confounder. *Journal of Causal Inference*, 9(1):229–249, 2021. doi: doi:10.1515/jci-2021-0033. URL <https://doi.org/10.1515/jci-2021-0033>.
- Thomas S Richardson and James M Robins. Single world intervention graphs (swigs): A unification of the counterfactual and graphical approaches to causality. *Center for the Statistics and the Social Sciences, University of Washington Series. Working Paper*, 128(30):2013, 2013.
- Donald B Rubin. Estimating causal effects of treatments in randomized and nonrandomized studies. *Journal of educational Psychology*, 66(5):688, 1974.
- Xu Shi, Wang Miao, Jennifer C. Nelson, and Eric J. Tchetgen Tchetgen. Multiply robust causal inference with double negative control adjustment for categorical unmeasured confounding, 2019.
- Xu Shi, Wang Miao, and Eric Tchetgen Tchetgen. A selective review of negative control methods in epidemiology. *Current Epidemiology Reports*, 7(4):190–202, DEC 2020. doi: 10.1007/s40471-020-00243-4.
- Ilya Shpitser, Zach Wood-Doughty, and Eric J. Tchetgen Tchetgen. The proximal id algorithm, 2023.
- Erik Sverdrup and Yifan Cui. Proximal causal learning of conditional average treatment effects, 2023.
- Eric J Tchetgen Tchetgen, Andrew Ying, Yifan Cui, Xu Shi, and Wang Miao. An introduction to proximal causal learning, 2020.
- Eric Tchetgen Tchetgen. The Control Outcome Calibration Approach for Causal Inference With Unobserved Confounding. *American Journal of Epidemiology*, 179(5):633–640, 12 2013. ISSN 0002-9262. doi: 10.1093/aje/kwt303. URL <https://doi.org/10.1093/aje/kwt303>.
- Carmen D Tekwe, Randy L Carter, Harry M Cullings, and Raymond J Carroll. Multiple indicators, multiple causes measurement error models. *Statistics in medicine*, 33(25):4469–4481, 2014.
- Ledyard R Tucker, Raymond F. Koopman, and Robert L. Linn. Evaluation of factor analytic research procedures by means of simulated correlation matrices. *Psychometrika*, 34(4):421–459, 1969. doi: 10.1007/BF02290601.
- Wouter AC van Amsterdam, Joost JC Verhoeff, Netanja I Harlianto, Gijs A Bartholomeus, Aahlad Manas Puli, Pim A de Jong, Tim Leiner, Anne SR van Lindert, Marinus JC Eijkemans, and Rajesh Ranganath. Individual treatment effect estimation in the presence of unobserved confounding using proxies: a cohort study in stage iii non-small cell lung cancer. *Scientific reports*, 12(1):5848, 2022.
- Stef van Buuren and Karin Groothuis-Oudshoorn. mice: Multivariate imputation by chained equations in r. *Journal of Statistical Software*, 45(3):1–67, 2011. doi: 10.18637/jss.v045.i03.
- Jingshu Wang, Qingyuan Zhao, Trevor Hastie, and Art B Owen. Confounder adjustment in multiple hypothesis testing. *Annals of statistics*, 45(5):1863, 2017.

A Identification Proofs

Proof of Theorem 1:

Proof. Suppose the relevant assumptions hold. For $a \in \mathcal{A}$, we have

$$\mathbb{E}[Y|Z, A = a, X] = \mathbb{E}[\mathbb{E}[Y|U, Z, A = a, X]|Z, A = a, X] \quad (1)$$

$$= \mathbb{E}[\mathbb{E}[Y(a)|U, Z, A = a, X]|Z, A = a, X] \quad (2)$$

$$= \mathbb{E}[\mathbb{E}[Y(a)|U, X]|Z, A = a, X] \quad (3)$$

using the law of iterated expectation, consistency, and conditional independence.

By Assumption 4.2, there exist $\tau(a, X)$ so that $\mathbb{E}[Y(a)|U, X] = \tau(a, X)g(U, X)$ for each $a \in \mathcal{A}$. Therefore,

$$\mathbb{E}[Y|Z, A = a, X] = \tau(a, X)\mathbb{E}[g(U, X)|Z, A = a, X].$$

Note that the left hand side is a function of the observed distribution, whereas

$\mathbb{E}[g(U, X)|Z, A = a, X]$ can be identified by the observed distribution by Assumption 4.1. Provided $\tau(a, X)$ is the unique solution to the above equation, then we can identify $\tau(a, X)$ from the observed distribution.

Then, consider

$$\begin{aligned} \mathbb{E}[Y(a)|Z, X] &= \mathbb{E}[\mathbb{E}[Y(a)|U, Z, X]|Z, X] \\ &= \mathbb{E}[\mathbb{E}[Y(a)|U, X]|Z, X] \\ &= \mathbb{E}[\tau(a, X)g(U, X)|Z, X] \\ &= \tau(a, X)\mathbb{E}[g(U, X)|Z, X]. \end{aligned}$$

The first step comes from the law of iterated expectation, the second from conditional independence, the third by Assumption 4.2, and finally by linearity of expectations. Again by linearity,

$$\mathbb{E}[Y(a) - Y(a')|Z = z, X] = (\tau(a, X) - \tau(a', X))\mathbb{E}[g(U)|Z = z, X].$$

It remains to argue that $\mathbb{E}[g(U, X)|Z = z, X]$ can be identified from the observed distribution. This comes from Assumption 4.1. Since $\mathbb{E}[g(U, X)|Z, A, X]$ can be identified from the observed distribution for (Z, A, X) , then $\mathbb{E}[g(U, X)|Z = z, X] = \mathbb{E}[\mathbb{E}[g(U, X)|Z = z, A, X]|Z = z, X]$ can be identified from the observed distribution as well. \square

B Multiple Indicators Multiple Causes Model Properties

Observation B.1. From the definitions of the MIMIC model, it must be true that

$$Z|U \sim MVN(\Lambda U + \nu, \Psi)$$

and

$$Z \sim MVN(\nu, \Lambda\Lambda' + \Psi).$$

We also have

$$\mathbb{E}[U|X] = \mathbb{E}[\Gamma X + \varepsilon_U|X] = \Gamma X$$

and

$$\mathbb{E}[(U - \Gamma X)(U - \Gamma X)'|X] = \mathbb{E}[\varepsilon_U\varepsilon_U'|X] = I.$$

For the moment, we reduce MIMIC to the usual factor analysis model by ignoring X .

Observation B.2. Let $A = b'U + c + \varepsilon_A$. If we augment the necessary matrices, we can write

$$\begin{bmatrix} Z \\ A \end{bmatrix} = \begin{bmatrix} \Lambda \\ b' \end{bmatrix} U + \begin{bmatrix} \nu \\ c \end{bmatrix} + \begin{bmatrix} \Psi^{1/2} \varepsilon_Z \\ \varepsilon_A \end{bmatrix}.$$

Therefore it must be true that

$$\begin{bmatrix} Z \\ A \end{bmatrix} | U \sim MVN \left(\begin{bmatrix} \Lambda \\ b' \end{bmatrix} U + \begin{bmatrix} \nu \\ c \end{bmatrix}, \begin{bmatrix} \Psi & \vec{0} \\ \vec{0}' & 1 \end{bmatrix} \right)$$

and

$$\begin{bmatrix} Z \\ A \end{bmatrix} \sim MVN \left(\begin{bmatrix} \nu \\ c \end{bmatrix}, \begin{bmatrix} \Lambda \\ b' \end{bmatrix} [\Lambda' \quad b] + \begin{bmatrix} \Psi & \vec{0} \\ \vec{0}' & 1 \end{bmatrix} \right)$$

where $\vec{0}$ is a $p \times 1$ vector of zeros.

We will denote the covariance matrix

$$\begin{bmatrix} \Psi & \vec{0} \\ \vec{0}' & 1 \end{bmatrix}$$

by Ψ^* .

Lemma B.1. Define $M := (\Lambda' \Psi^{-1} \Lambda + I)$. If Λ is full rank, M is invertible.

Proof. We will show $\Lambda' \Psi^{-1} \Lambda$ is positive definite since the sum of positive definite matrices is also positive definite, and therefore invertible. Clearly $\Lambda' \Psi^{-1} \Lambda$ is symmetric. As an invertible covariance matrix, Ψ must be positive definite. The inverse must also be positive definite since the inverse of the eigenvalues of a matrix are the eigenvalues of the matrix inverse. Since Λ is full rank, $\Lambda v = 0$ if and only if v is the zero vector. For a nonzero vector $v \in \mathbb{R}^k$,

$$v' \Lambda' \Psi^{-1} \Lambda v = (\Lambda v)' \Psi^{-1} (\Lambda v) > 0$$

since $\Lambda v \neq 0$ and Ψ^{-1} is positive definite. □

Lemma B.2. Let $U \sim MVN(0, I) \in \mathbb{R}^k$, and $Z|U \sim MVN(\Lambda U + \nu, \Psi) \in \mathbb{R}^p$. Fix $z \in \mathbb{R}^p$ and let $d := \Lambda' \Psi^{-1} (z - \nu)$. If $M := (\Lambda' \Psi^{-1} \Lambda + I)$ is invertible, then

$$U|Z = z \sim MVN(M^{-1}d, M^{-1}).$$

Proof. Since Z and U have densities, we can consider $f_{U|Z=z}(u) = f_{Z|U=u}(z) f_U(u) / f_Z(z)$ using Bayes rule. Then, up to a constant in z ,

$$\begin{aligned} \frac{f_{Z|U=u}(z) f_U(u)}{f_Z(z)} &\propto \exp \left(-\frac{1}{2} (z - \Lambda u - \nu)' \Psi^{-1} (z - \Lambda u - \nu) \right) \exp \left(-\frac{1}{2} u' u \right) \\ &= \exp \left(-\frac{1}{2} ((z - \nu)' \Psi^{-1} (z - \nu) + u' (\Lambda' \Psi^{-1} \Lambda + I) u - 2(z - \nu)' \Psi^{-1} \Lambda u) \right) \\ &\propto \exp \left(-\frac{1}{2} (u - M^{-1}d)' M (u - M^{-1}d) \right) \end{aligned}$$

□

Using the matrix augmentation from Observation B.2, we arrive at the following corollary.

Corollary B.1. Let $A = b'U + c + \varepsilon_A$ where U, b, c, ε_A , and Z are defined as in Assumption 4.3. If $M^* = [\Lambda' \quad b] (\Psi^*)^{-1} \begin{bmatrix} \Lambda \\ b' \end{bmatrix} + I$ is invertible then $U|Z = z, A = a \sim MVN((M^*)^{-1}d^*, (M^*)^{-1})$ where $d^* = [\Lambda' \quad b] (\Psi^*)^{-1} \begin{bmatrix} z - \nu \\ a - c \end{bmatrix}$.

We can compute $U|Z, X$ for the MIMIC model in a similar manner to the computation for $U|Z$ above. We have

$$f_{U|Z, X}(u) = \frac{f_{U, Z, X}(u, z, x)}{f_{Z, X}(z, x)} = \frac{f_{Z|U}(z)f_{U|X}(u)f_X(x)}{f_{Z|X}(z)f_X(x)} = \frac{f_{Z|U}(z)f_{U|X}(u)}{f_{Z|X}(z)} \propto f_{Z|U}(z)f_{U|X}(u).$$

Therefore

$$\begin{aligned} f_{U|Z, X}(u) &\propto \exp\left(-\frac{1}{2}[(z - \Lambda U - \nu)' \Psi^{-1}(z - \Lambda U - \nu) + (U - \Gamma X)'(U - \Gamma X)]\right) \\ &\propto \exp\left(-\frac{1}{2}[U' \Lambda' \Psi^{-1} \Lambda U - 2(z - \nu)' \Psi^{-1} \Lambda U + U' U - 2X' \Gamma' U]\right) \\ &\propto \exp\left(-\frac{1}{2}[U'(\Lambda' \Psi^{-1} \Lambda + I)U - 2((z - \nu)' \Psi^{-1} \Lambda + X' \Gamma') U]\right) \\ &\propto \exp\left(-\frac{1}{2}(U' M U - 2(d' + X' \Gamma') U)\right) \\ &\propto \exp\left(-\frac{1}{2}(U - M^{-1}(d + \Gamma X))' M (U - M^{-1}(d + \Gamma X))\right) \end{aligned}$$

so $U|Z, X \sim MVN(M^{-1}(d + \Gamma X), M^{-1})$.

Similarly to the process for incorporating A previously, if we augment our matrices we can show that $U|Z, X, A \sim MVN((M^*)^{-1}(d^* + \Gamma X), (M^*)^{-1})$.

C Simulated Data Robustness Checks

Implementations are available at

<https://github.com/HaleyColgateKottler/LatentProxyVars>.

Comparison methods

We provide R code used for the comparison methods to enable replication. Each function requires a dataframe of observations of Z, A, Y .

We use a modification of the usual IPW algorithm to allow for continuous treatments. Note that for binary treatments we use the usual IPW algorithm with logistic regression.

```
continuousIPWest <- function(df) {
  AZ <- subset(df, select = -c(Y))
  Z <- subset(AZ, select = -c(A))

  m1 <- glm(formula = A ~ ., family = gaussian(link = "identity"), data = AZ)
  meanAZ <- predict(m1, newdata = Z, type = "response")
  varAZ <- var(df$A - meanAZ)
  weightings <- dnorm(df$A, mean = meanAZ, sd = sqrt(varAZ))

  m2 <- glm(formula = A ~ 1, family = gaussian(link = "identity"), data = AZ)
  meanA <- predict(m2, newdata = df, type = "response")
  varA <- var(df$A - meanA)
  numerators <- dnorm(df$A, mean = meanA, sd = sqrt(varA))

  df$full.weights <- numerators / weightings
  df$A2 <- df$A^2
  design <- svydesign(
```

```

    id = ~1,
    weights = ~full.weights,
    data = df
  )

m3 <- svyglm(
  formula = formula(paste("Y ~ A + A2 + ",
    paste0(colnames(Z), collapse = " +"))),
  family = gaussian(link = "identity"),
  data = df, design = design)

newdata1 <- data.frame("A" = 1, Z, "A2" = 1)
EY1 <- mean(predict(m3, newdata1))
newdata0 <- data.frame("A" = 0, Z, "A2" = 0)
EY0 <- mean(predict(m3, newdata0))

return(EY1 - EY0)
}

```

We use a simple linear model for Y in terms of A and Z , and extract the coefficient on A for the ATE estimate.

```

linearEst <- function(df) {
  m1 <- lm(Y ~ ., df)
  linear.ATE <- m1$coefficients["A"]

  return(linear.ATE)
}

```

For proximal causal inference, you must additionally provide lists of the NCOs and NCEs that are included in the dataframe.

```

proximal_causal <- function(df, nco.names, nce.names){
  wformulas <- paste(nco.names,
    " ~ A + ", paste0(nce.names, sep = "",
      collapse = " + "),
    " + ", paste0("A * ", nce.names, sep = "",
      collapse = " + "), sep = "")
  m.hW <- lapply(wformulas, lm, data = df)
  wav <- sapply(m.hW, predict, data = df[,c("A", "Y", nce.names)])

  prior.names <- colnames(df)
  df <- cbind(df, wav)
  colnames(df) <- c(prior.names,
    paste("wav", 1:length(nco.names), sep = ""))

  # estimate tau_a
  m1formula <- paste("Y ~ A + ",
    paste0("wav", 1:length(nco.names), collapse = " + "),
    " + ",
    paste0("A * ", paste("wav", 1:length(nco.names),
      sep = ""), collapse = " + "),
    sep = "")
}

```

```

m1 <- lm(m1formula, df)
alpha <- m1$coefficients[c("(Intercept)",
                          paste("wav", 1:length(nco.names), sep = ""))]
gamma <- m1$coefficients[c("A", paste("A:wav", 1:length(nco.names),
                                      sep = ""))]

# calc CATE
mWVformulas <- paste(nco.names,
                    " ~ ", paste0(nce.names, collapse = " + "))
m.WVs <- lapply(mWVformulas, lm, data = df)
WVs <- lapply(m.WVs, predict, data = df)
CATE <- gamma[1] + gamma[2:(1 + length(nco.names))] %*%
      t(sapply(WVs, unlist))
return(mean(CATE))
}

```

We implement a standard IV algorithm.

```

IVest <- function(df) {
  AZ <- subset(df, select = -c(Y))

  m1 <- lm(formula = A ~ ., data = AZ)
  df$x <- predict(m1, newdata = df)

  m2 <- lm(formula = Y ~ x, data = df)

  IV_ATE <- m2$coefficients[["x"]]
  return(IV_ATE)
}

```

Parameters

These are the parameters used for the synthetic data robustness study.

Consistency

. Following the model introduced in Section 4.2, data is generated using $k = 2$, $p = 8$, $\nu = \overline{0}$,

$$\lambda = \begin{bmatrix} 0.534 & -0.644 \\ 0.000 & 0.837 \\ 0.425 & 0.648 \\ 0.207 & 0.811 \\ -0.103 & 0.889 \\ -0.020 & 0.774 \\ 0.256 & 0.797 \\ 0.894 & -0.015 \end{bmatrix}$$

$$\text{diag}(\psi) = [0.548, 0.548, 0.632, 0.548, 0.447, 0.632, 0.548, 0.447]$$

$$b = [-0.113, 0.829], c = 0.2$$

$$Y = \left(\begin{bmatrix} -0.8 \\ 0.5 \\ -0.9 \end{bmatrix} + A \begin{bmatrix} 0.3 \\ 0.9 \\ 0.4 \end{bmatrix} \right) \begin{bmatrix} 1 \\ U \end{bmatrix} + \varepsilon_Y \text{ where } \varepsilon_Y \sim \mathcal{N}(0, 0.1)$$

IV

. For this test, $U \sim \mathcal{N}(0, I) \in \mathbb{R}^2$ and $Z \sim \mathcal{N}(0, I) \in \mathbb{R}^6$. The treatment assignment is generated via $A = \Lambda \begin{bmatrix} Z \\ U \end{bmatrix} + \varepsilon_A$ where $\varepsilon_A \sim \mathcal{N}(0, 1)$. Then

$$Y = (\alpha + A\gamma) \begin{bmatrix} 1 \\ U \end{bmatrix} + \varepsilon_Y$$

where $\varepsilon_Y \sim \mathcal{N}(0, 0.1)$. Additionally, $\Lambda = [0.245, 0.614, 0.272, 0.140, 0.002, -0.007, -0.013, 0.263]$, $\alpha = [-0.6, 0.2, 0.7]$, and $\gamma = [0.3, 0.8, 0.4]$.

No latent variable

. For this test, $Z \sim \mathcal{N}(0, \Psi) \in \mathbb{R}^6$, where

$$\text{diag}(\Psi) = [0.548, 0.632, 0.548, 0.447, 0.632, 0.4472136, 0.632, 0.447].$$

Then $A = \Lambda Z + \varepsilon_A$ where $\varepsilon_A \sim \mathcal{N}(0, 1)$ and

$$\Lambda = [0.002, 0.692, 0.004, 0.347, -0.014, 0.005, 0.000, 0.008].$$

Finally, $Y = (\alpha + A\gamma) \begin{bmatrix} 1 \\ Z \end{bmatrix} + \varepsilon_Y$ with $\varepsilon_Y \sim \mathcal{N}(0, 0.01)$,

$$\alpha = [-0.9, 0.7, 0.6, -0.6, 0.8, 0.3, 0.2, -0.5, 0.4] \text{ and}$$

$$\gamma = [0.3, 0.4, 0.7, 0.5, 0.2, -0.8, -0.7, 0.9, -0.6].$$

Skew normal

. This test followed the model from Section 4.2 except that $U \in \mathbb{R}$ is skew normal with shape parameter 5, location parameter -1.26 , and scale parameter 1.606. Additionally,

$$\Lambda = [0.632, 0.548, -0.548, 0.632, 0.548],$$

$$\text{diag}(\Psi) = [0.775, 0.837, 0.837, 0.775, 0.837],$$

$$b = -0.632, c = 0.2, \text{ and } Y = ([-0.9, 0.7] + A[0.3, 0.6]) \begin{bmatrix} 1 \\ U \end{bmatrix} + \varepsilon_Y \text{ where } \varepsilon_Y \sim \mathcal{N}(0, 0.001).$$

Binary A

. For U and Z , this followed the model from Section 4.2. The treatment was generated with a probit model via

$$A = \begin{cases} 1 & \text{if } b'U + c + \varepsilon_A \\ 0 & \text{otherwise} \end{cases}$$

where $\varepsilon_A \sim \mathcal{N}(0, 1)$. Here $k = 3$, $p = 10$,

$$\Lambda = \begin{bmatrix} -0.033 & 0.104 & 0.830 \\ -0.027 & 0.544 & 0.062 \\ -0.042 & 0.494 & 0.674 \\ 0.465 & -0.041 & 0.531 \\ -0.017 & 0.332 & 0.436 \\ 0.142 & 0.035 & 0.528 \\ 0.058 & 0.169 & 0.518 \\ 0.256 & 0.026 & 0.796 \\ 0.095 & 0.196 & 0.808 \\ 0.038 & 0.293 & 0.783 \end{bmatrix},$$

$$\text{diag}(\Psi) = [0.548, 0.837, 0.548, 0.707, 0.837, 0.837, 0.837, 0.548, 0.548, 0.548],$$

$b = [0.242, 0.039, 0.490]$, and $c = 0.2$. Finally,

$$Y = ([0.7, 0.5, 0.6, -0.4] + A[0.3, 0.9, -0.8, 0.2]) \begin{bmatrix} 1 \\ U \end{bmatrix} + \varepsilon_Y \text{ where } \varepsilon_Y \sim \mathcal{N}(0, 0.01).$$

Ratio of number of proxies to dimension of latent variable

. For this test, data generation followed the model from Section 4.2 with $k = 2$. To allow for increasing numbers of proxies, parameters were chosen for $p = 20$, and then truncated as necessary for smaller p values. We used

$$\begin{aligned} \text{diag}(\Psi) = [0.894, 0.894, 0.837, 0.775, 0.775, 0.837, \\ 0.837, 0.837, 0.894, 0.894, 0.894, 0.894, \\ 0.775, 0.837, 0.837, 0.775, 0.894, 0.894, 0.894] \end{aligned}$$

, $b = [0.044, 0.631]$, $c = 0$,

$$Y = ([-0.7, -1.9, 1.3] + A[0.3, -0.2, 0.0]) \begin{bmatrix} 1 \\ U \end{bmatrix} + \varepsilon_Y \text{ where } \varepsilon_Y \sim \mathcal{N}(0, 0.1), \text{ and}$$

$$\Lambda = \begin{bmatrix} 0.436 & 0.098 \\ 0.445 & 0.048 \\ 0.515 & 0.188 \\ -0.054 & 0.630 \\ -0.031 & 0.632 \\ 0.548 & -0.009 \\ 0.544 & 0.064 \\ 0.542 & 0.079 \\ -0.038 & 0.446 \\ 0.435 & 0.106 \\ 0.435 & 0.102 \\ 0.191 & 0.404 \\ 0.447 & 0.013 \\ -0.016 & 0.632 \\ 0.534 & 0.120 \\ -0.037 & 0.546 \\ 0.290 & 0.562 \\ 0.144 & 0.423 \\ -0.038 & 0.446 \\ 0.446 & -0.035 \end{bmatrix}.$$

Higher order outcome generation models

. Data generation for (U, Z, A) followed Section 4.2 with $k = 1$, $p = 6$,

$$\Lambda = \begin{bmatrix} -0.775 \\ -0.894 \\ 0.775 \\ 0.775 \\ -0.775 \\ -0.775 \end{bmatrix},$$

$$\text{diag}(\Psi) = [0.632, 0.447, 0.632, 0.632, 0.632, 0.632],$$

$b = 0.837$ and $c = 0$. Finally,

$$Y = ([0.5, 0.7, -0.8] + A[-0.4, -0.9, 0.7]) \begin{bmatrix} 1 \\ U \\ U^2 \end{bmatrix} + \varepsilon_Y \text{ with } \varepsilon_Y \sim \mathcal{N}(0, 0.1).$$

Coverage

. Following the model in Section 4.2, data was generated with $p = 6$ and $k = 2$ using

$$\Lambda = \begin{bmatrix} 0.498 & 0.673 \\ -0.099 & 0.768 \\ 0.886 & -0.125 \\ 0.600 & -0.490 \\ -0.617 & 0.566 \\ 0.326 & 0.833 \end{bmatrix},$$

$$\text{diag}(\Psi) = [0.548, 0.632, 0.447, 0.632, 0.548, 0.447],$$

$b = [0.833, -0.078]$ and $c = 0$. Finally,

$$Y = ([0.7, -0.5, -0.8] + A[0.5, 0.7, 0.2]) \begin{bmatrix} 1 \\ U \end{bmatrix} + \varepsilon_Y \text{ where } \varepsilon_Y \sim \mathcal{N}(0, 0.1).$$

Results with Comparison to the Instrument Variables Method

Since instrument variable techniques are very sensitive to assumptions, the resulting estimates are often orders of magnitude different from other methods. However, for completeness we include those in Figure 5 and .

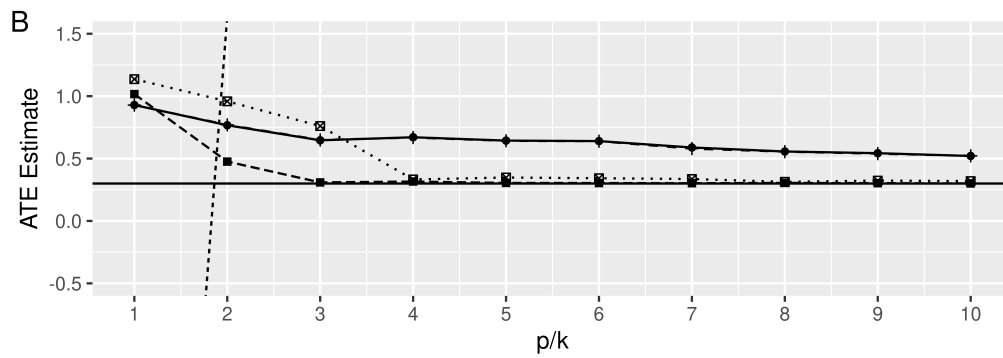
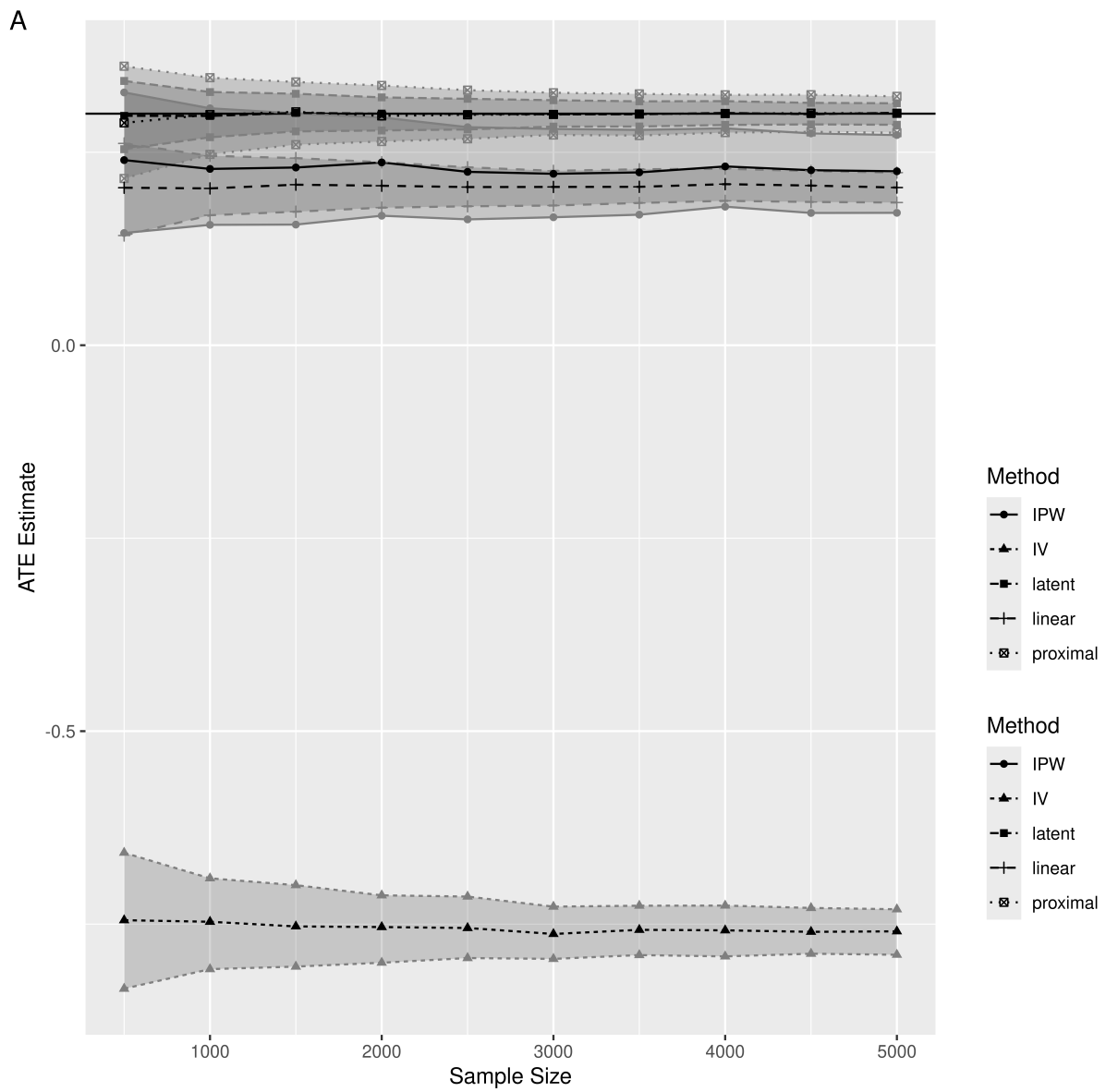


Figure 5: Robustness results

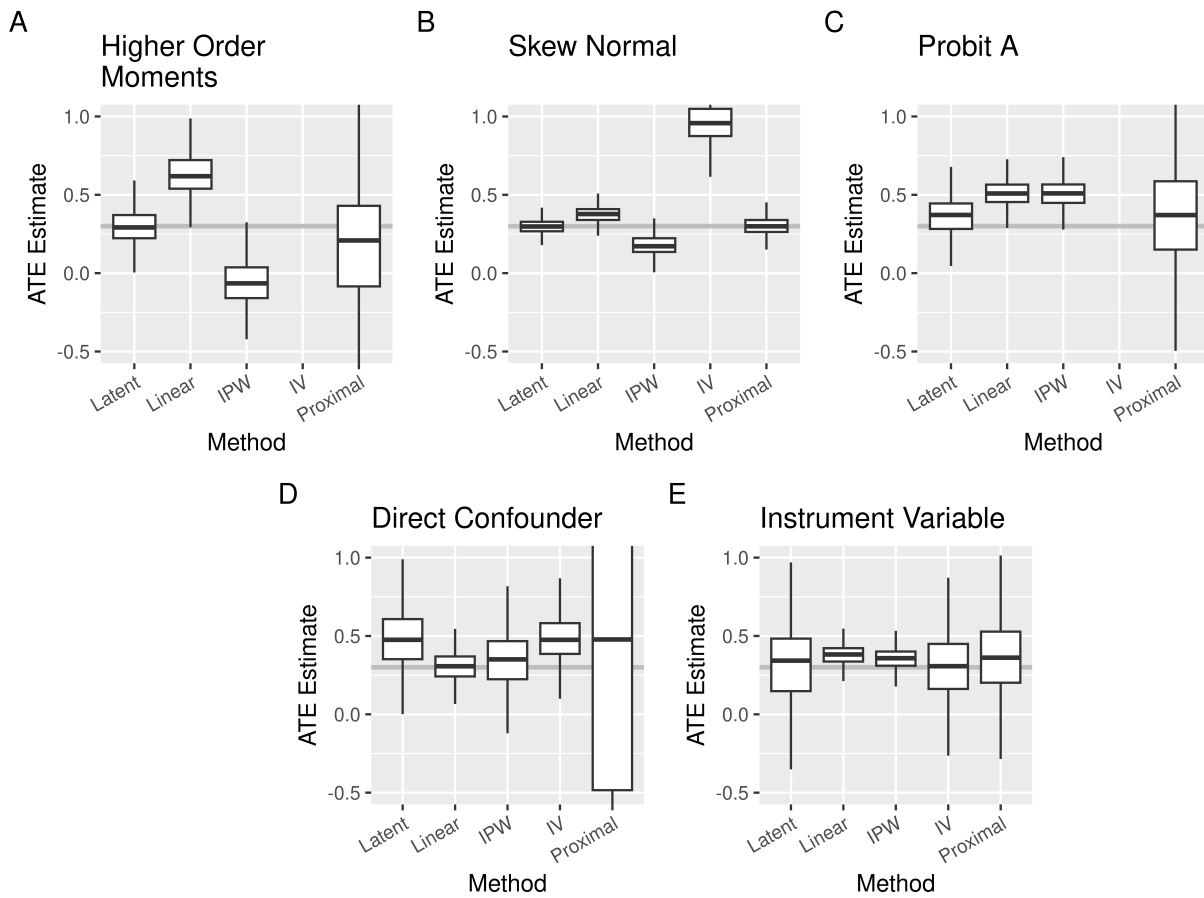


Figure 6: Robustness results